**Atmospheric
Chemistry
and Physics
Discussions**

**Sea ice, frost flowers
and halogen
activation**

W. R. Simpson et al.

EGU

First-year sea-ice contact predicts bromine monoxide (BrO) levels better than potential frost flower contact

W. R. Simpson[1], D. Carlson[1], G. Hoenninger[1,2,†], T. A. Douglas[3], M. Sturm[3], D. Perovich[3], and U. Platt[2]

[1]Geophysical Institute and Department of Chemistry, University of Alaska Fairbanks, Fairbanks, AK 99775-6160, USA
[2]Institute for Environmental Physics, University of Heidelberg, Im Neuenheimer Feld 229, 69120 Heidelberg, Germany
[3]U.S. Army Cold Regions Research and Engineering Laboratory, P.O. Box 35170, Fort Wainwright, AK 99703-0170, USA
[†]deceased

Correspondence to: W. R. Simpson (ffwrs@uaf.edu)

Sea ice, frost flowers and halogen activation

W. R. Simpson et al.

EGU

Abstract

Reactive halogens are responsible for boundary-layer ozone depletion and mercury deposition in Polar Regions during springtime. To investigate the source of reactive halogens in the air arriving at Barrow, Alaska, we measured BrO, a marker of reactive halogen chemistry, and correlated its abundance with airmass histories derived from meteorological back trajectories and remotely sensed sea ice properties. The BrO is found to be positively correlated to first-year sea-ice contact (R^2=0.55), and weakly negatively correlated to potential frost flower (PFF) contact (R^2=0.04). These data indicate that snow contaminated with sea salts on first-year sea ice is a more probable bromine source than are frost flowers. Recent climate-driven changes in Arctic sea ice are likely to alter frost flower and first year sea ice prevalence, suggesting a significant change in reactive halogen abundance, which will alter the chemistry of the overlying Arctic atmosphere.

1 Introduction

During late winter and spring, oxidation chemistry in the Arctic troposphere shifts from being dominated by ozone photochemistry to being dominated by halogen chemistry, especially reactive bromine chemistry. This shift has profound influences that range from depletion of tropospheric ozone to deposition of mercury to alteration of the fate and lifetime of organic pollutants (Barrie et al., 1988; Schroeder et al., 1998). The majority of the bromine atoms responsible for ozone depletion and mercury deposition come from salts containing bromide (Br-) that originate from the ocean and are oxidized to bromine atomic radicals through an autocatalytic reaction pathway known as the bromine explosion (Fan and Jacob, 1992; McConnell et al., 1992). The transfer mechanism by which the salts become atmospherically accessible is not currently understood, yet this mechanism plays a fundamental role in activating halogens that deposit airborne contaminants (e.g. Hg) to the terrestrial cryosphere.

Two hypotheses have been presented for the mechanism of bromide salt transport from the ocean to reactive bromine in the atmosphere. Frost flowers, which are highly saline, have been proposed to provide the surface from which bromine is released (Rankin et al., 2002). Kaleschke et al. (2004) and co-workers used remotely sensed sea ice data to predict where frost flowers may be forming on sea ice. They introduced a proxy they called potential frost flowers (PFF), which is calculated by a thermodynamic model of sea ice and frost flower growth and found that PFF is correlated with BrO detected by satellite (Kaleschke et al., 2004). Jones et al. (2006) found that ozone depletion events detected at Halley Bay, Antarctica were correlated with airmass motions that brought air in contact with a large coastal polyna that often produces frost flowers. Snow contaminated with salts, which are prevalent on first-year sea ice, has also been proposed to be the surface from which bromine is released. Direct mass-spectroscopic evidence of release of Br_2 and $BrCl$ (precursors of BrO) from snow (Foster et al., 2001), and depletions of Br- in coastal snow (Simpson et al., 2005) provide evidence for the salty snow hypothesis. Satellite observations (Wagner et al., 2001) and ground-based observations of BrO in Antarctica (Frieß et al., 2004) also point to first-year ice as an important region for bromine activation.

Freezing sea water separates ice from brine, which is a concentrated salt solution. Some of this brine is forced to the new ice surface, causing high initial surface salinities of 50–100 parts per thousand by weight (‰, where Arctic Ocean sea-water salinity ≈30‰). As the ice ages, the surface salinity decreases to approximately 5–10‰. Snow on the sea ice is contaminated by salts when brine wicks up the snow or the wind scours the snow to re-expose saline surfaces or salt aerosols deposit to the snow (Domine et al., 2004). Sea ice that survives the summer has a much lower surface salinity because the brine drains away during summer melting. Therefore, multi-year sea ice (MYI) and land surfaces contain less atmospherically accessible salt and are less likely to be reactive halogen sources than first-year sea ice (FYI). Frost flowers form when open leads or polynyas freeze over and small nodules in the forming ice act as condensation nuclei for vapor deposition of angular ice crystals that look like deli-

cate flowers. The flowers wick brine from the sea-ice surface producing highly saline (≈100‰) crystals with specific surface areas similar to that of surface hoar (Domine et al., 2005; Perovich and Richter-Menge, 1994).

2   Methods

₅ The contact time of an air parcel with potential frost flowers (PFF) or first-year ice (FYI) is calculated by combining back-trajectory analysis, which provides air motion and temperature with remotely sensed sea ice data, which provides information on where open water and ice are present. In the PFF calculation, open water is assumed to be freezing over and producing new frost flowers with increasing efficiency as the
₁₀ temperature decreases (Kaleschke et al., 2004). Figure 1 shows an example of this calculation where a trajectory passes near a coastal polynya in the vicinity of Banks Island, Canada.

2.1   PFF calculation

For each hour during the winter/spring of 2005, we calculate a 72 h back trajectory
₁₅ at 50 m arrival height using the HYSPLIT trajectory model (Draxler and Rolph, 2003). In the time period shown (DOY 80–120), there are 960 total trajectories considered. Other arrival heights (of 100 and 300 m) were explored and shown to have similar results. The open water fraction, assumed to be 1 – sea ice concentration, comes from ASI algorithm (Kaleschke et al., 2001) sea-ice maps (based upon AMSR-E data) at the
₂₀ 6.25 km resolution downloaded from http://www.seaice.de/. Airmasses are propagated back along the prescribed trajectory and minutes of contact with open water are calculated on a pixel-by-pixel basis using the appropriate daily sea-ice map. For example, if the trajectory spends 30 min in a particular pixel, and the sea-ice fraction is 66% in that pixel, then there are $(1-0.66) \times 30$ min $= 10$ min of open water contact for this pixel. We
₂₅ then use the PFF parameterization (Kaleschke et al., 2004) based upon the parcel's

EGU

temperature to calculate the percent of open water that could maximally be covered by frost flowers. Continuing the example, say the PFF parameterization indicates 50% PFF coverage. We then multiply the 10 min in this pixel by 0.5 to get 5 min of PFF contact. The PFF contact is then summed over the entire 72 h trajectory to get the total

5 PFF contact for the airmass arriving at Barrow at the arrival time. If the trajectory goes over 1 km height, it is assumed to no longer have sea-ice contact. This 1 km height was chosen as a typical height of the convective cloud that would be in the presence of a lead.

Airmass dispersion occurs in the atmosphere but is not accounted for in the trajec-
10 tory calculation. Additionally, inaccurate meteorological fields cause back trajectory errors. Therefore, we added a feature to the calculation where the average sea ice concentration in a circle centered at the trajectory's calculated position is used instead of simply the immediate pixel of the calculated position. This circle increases in radius as time is propagated backwards at 2 km/hr. This "diffusion" rate is about 1/10th of the
15 wind speed and results in a radius of ≈140 km three days before arrival. Substituting this algorithm for the simple pixel-by-pixel calculation smoothed some high-frequency noise in the PFF time series, and was chosen as more realistic. In the example shown in Fig. 1, the PFF contact is with the polynya areas near Banks Island, Canada and arises from the radial averaging algorithm causing overlap of the trajectory with the
20 open water shown in that vicinity.

We performed many tests where the recently past sea ice conditions (up to 5 days earlier) were considered instead of the current sea-ice conditions. The idea of these tests was to see if frost flowers that may have formed a few days before the trajec-tory passed over a pixel were responsible for halogen activation. None of these tests
25 showed significantly better correlation with BrO, and thus we present the results using the formulation used by Kaleschke et al. (2004) because it has been accepted in the literature.

Printer-friendly Version

Interactive Discussion

2.2 First-year sea-ice contact calculation

First year ice (FYI) contact is calculated in a similar manner along the same trajectories, following the method of Frieß et al. (2004). Regions of older ice (second year or older) were identified through examination of QuikSCAT sea ice backscatter coefficient, which is a proxy for sea ice age (Voss et al., 2003). The QuikSCAT data were downloaded from http://www.ifremer.fr/. We found that the region of older ice is relatively stationary during the 40-day period of analysis. Therefore, one mask of old sea ice, shown in yellow in Fig. 1, was generated from the observation on DOY 100 (10 April 2005). With this mask, we identify regions of first-year sea ice and sum the ice fraction times the contact time for each pixel along the trajectory. If the trajectory indicates that the parcel is at an altitude over 100 m (twice the 50 m arrival height), we consider the contact with the surface is lost and do not accumulate any first-year sea-ice contact.

2.3 Chemical measurements

Bromine monoxide (BrO) and ozone were measured continually at Barrow, Alaska (71.3 N, 156.7 W) over the winter and spring of 2005. Bromine monoxide was measured by multiple-axis differential optical absorption spectroscopy (MAX-DOAS) (Hoenninger and Platt, 2002). Measurements were made at multiple viewing elevations to separate stratospheric BrO from tropospheric BrO and to derive vertical profiles of the BrO concentration. Strict inversion of the data to concentration profiles is complicated by radiation transfer issues. Therefore, we chose the difference in slant column density (DSCD) of BrO between a 2-degree elevation angle measurement and a near-coincident zenith measurement to quantify the tropospheric BrO abundance. The high degree of correlation shown in this work argues for the accuracy of this simple quantification of BrO. For clear-sky conditions, 10^{14} molecule cm^{-2} DSCD corresponds to about a 5 parts per trillion by volume (pptv) mixing ratio in a 1 km thick mixed layer. The peak values shown here are $\approx$30 pptv, which is similar to values seen at other Arctic locations where halogen activation is prevalent (Hausmann and Platt, 1994; Hoenninger

EGU

and Platt, 2002; Tuckermann et al., 1997). Hourly in-situ ozone mixing ratios were measured by the National Oceanic and Atmospheric Administration (NOAA) Earth Systems Research Laboratory/Global Monitoring Division (ESRL/GMD).

3 Results

Figure 2 shows time series of ozone, BrO, FYI contact, and PFF contact for Barrow, Alaska. Ozone and BrO are generally anticorrelated, as expected because BrO destroys ozone. Because it requires time for BrO to destroy ozone, the anticorrelation is not precise, and BrO is considered a better marker of halogen activation. The BrO data follow the FYI contact remarkably well, particularly the rapid variations during the period DOY 110 to 119. In contrast, the BrO shows little relationship to PFF. The largest BrO events (DOY 110 to 112) occur after very little PFF contact, while the largest PFF contact event, DOY 115, is correlated with essentially no BrO. Therefore, PFF appears unrelated to BrO.

There are two days where FYI contact is high but BrO is near zero, DOY 88 and 97. Both of these days have extremely low ozone, nearly always <1 ppbv, as indicated by the red coloring of all BrO data when O_3<1 ppbv. At these low ozone levels, reactive bromine (the sum of the concentrations of Br and BrO) partitions to Br atoms because the ozone necessary to form BrO is absent. Therefore, the absence of BrO on DOY 88 and 97 is expected, and we exclude these data from later analysis.

Figure 3 shows the correlations of BrO with FYI and BrO with PFF contact. BrO is positively correlated with FYI contact while BrO is weakly anticorrelated with PFF. Although the functional form of the relationship between BrO and FYI is unknown, a simple linear model appears to fit well and can explain 55% of the variance in BrO (R^2=0.55). This correlation is quite impressive given inaccuracies in the trajectory model and inevitable variations in other important meteorological parameters, such as wind speed and inversion height. On the other hand, a linear model of the dependence of BrO on PFF can explain <5% of the variance (R^2=0.04), and the slope of the

EGU

correlation is opposite to the expectation that PFF should produce BrO. The intercept of this correlation, which indicates significant BrO in the absence of PFF contact also does not make sense. These findings clearly indicate that contact with first-year sea ice provides the majority of reactive bromine to airmasses that arrive at Barrow during the ozone depletion season.

4 Discussion

The potential frost flower algorithm was chosen for this work because Kaleschke et al. (2004) reported that PFF from large polynya areas spatially matched regions of enhanced BrO detected by satellite. In the Kaleschke study, PFF came mostly from large coastal polynyas because those areas are a major source of open water in the Polar Regions. In our study, we also find that most airmasses with high PFF contacts can be traced to coastal polynyas or leads. Although there is commonly a lead a few kilometers from Barrow, this lead opens when winds drive ice away from the shore, and this lead seldom affects airmasses that blow onshore to the Barrow site. Therefore, the leads/polynyas that contribute to PFF typically impact the airmass days before arrival at Barrow and the overall PFF contact time is quite low. If the influence of polynyas/leads occurs relatively local to the source, their influence could have diminished before airmasses impact Barrow, which might explain the lack of correlation seen here. If it is the case that PFF produces only a local effect, then there must be another source of reactive bromine, associated with sea ice, to explain the high levels of BrO observed at Barrow in this study.

In the Jones et al. (2006) study, ozone depletion was observed when airmasses passed over a coastal polyna, which they interpreted as being covered by frost flowers and these frost flowers providing reactive bromine to deplete the ozone. The trajectories shown in the Jones et al. paper also pass across areas of first-year sea ice before traversing the coastal polynya, so it is possible that a sea-ice source of bromine caused their ozone depletions instead of the interpretation that frost flowers caused the ozone

W. R. Simpson et al.

EGU

depletion. In our analysis of data arriving at Barrow, the different mechanisms of PFF contact and FYI contact allow the PFF and FYI contact time series to be very different and allow separation of the sources. It is unclear from the Jones et al. analysis whether potential frost flower contact and first-year sea-ice contacts are different in their data. Therefore, we cannot speculate on whether their data uniquely point to frost flowers as the source of reactive bromine, but simply note that their data probably could be alternatively interpreted as due to first-year sea-ice contact.

Our study clearly shows that first-year sea ice is correlated with reactive halogen production, but we need to consider what specific property of these geographic areas is responsible for the halogen production. Ice motion, even in the middle of the pack, causes cracks to form such that on the order of a percent of the ice area is open water. Given cold temperatures, these open leads freeze over, forming surface brine. Frost flower formation additionally requires supersaturated water vapor, which depends on the presence of nearby open leads to source the water vapor (Andreas et al., 2002). Because small leads may be difficult to detect by satellite remote sensing, we cannot preclude the possibility that some frost flowers have formed in the first-year ice even though the calculated PFF contact is very small for these trajectories. As brine and frost-flower covered areas age, on the time scale of a few days, they may be covered by snow or the frost flowers could be blown away by wind (Perovich and Richter-Menge, 1994). Therefore, frost flower formation is temporally transient in addition to being spatially limited. The property of frost flowers thought to make up for these limiting factors is their specific surface area (the ice surface area per mass), which was initially estimated to be very large (Rankin et al., 2002). However, the specific surface area of frost flowers has recently been shown to be much smaller and similar to that of snow (Domine et al., 2005), making frost flowers appear less likely as the bromine source. Overall, frost flowers that may be present in the first-year ice would only provide a saline surface over small areas and for short periods of time.

Snow contaminated by salts is ubiquitous in the FYI area. Snow on sea ice has a wide distribution of depths and large areas are only covered by shallow snow that can

Sea ice, frost flowers and halogen activation

W. R. Simpson et al.

be influenced by brine wicking from the sea ice surface. Snow on FYI is also shallower (mean depth 20 cm) and less prevalent than snow on MYI (Sturm et al., 2002). Studies from Antarctica have shown snow salinities of 5‰ commonly occur at heights up to 20 cm in the snow pack (Massom et al., 2001), and summertime measurements from the Arctic show highly variable snow salinity with an average of 1‰ that may have been reduced by summer brine drainage (Eicken et al., 2002). Wind pumping of air through snow also increases the depth within the snowpack to which sea salts can become atmospherically accessible. Frost flowers could produce aerosols that contaminate the snow surface and this snow could later release bromine, leading to correlation with first-year sea-ice but not PFF. From these observations, we find that saline snow on the first-year sea ice is ubiquitous and contains significant quantities of salts necessary for halogen activation. Therefore, the common source of salty snow appears more likely than the transient and spatially limited frost flowers that may have formed but have been undetected by the PFF method.

5 Conclusions

Potential frost flower contact time, as calculated by meteorological back trajectories and remotely sensed sea ice features is not well correlated to BrO arriving at Barrow, while first-year sea-ice contact is positively correlated to BrO. These data point to first-year sea ice areas as the major source region for reactive bromine arriving at Barrow during the ozone depletion season with salty snow apparently being the bromine source mechanism. The Arctic has recently seen dramatic reductions in sea ice coverage and increases in air temperatures, with most models predicting further ice losses (Johannessen et al., 1999; Overpeck et al., 2005; Serreze et al., 2003; Stroeve et al., 2005). This marked modification of sea ice coverage is likely to have different effects on formation of first-year sea ice and frost flowers. For example, a warmer Arctic with less summer sea ice might have less frost flowers in spring due to warmer temperatures but more saline snow on first-year sea ice. A better mechanistic understanding of

EGU

the relative global importance of these two possible reactive bromine sources is critical for meaningful prediction of future halogen activation, boundary-layer ozone depletion, and mercury deposition in the context of a rapidly changing Arctic.

References

Andreas, E. L., Guest, P. S., Persson, P. O. G., Fairall, C. W., Horst, T. W., Moritz, R. E., and Semmer, S. R.: Near-surface water vapor over polar sea ice is always near ice saturation, J. Geophys. Res., 107, SHE 8–1, 2002. 11059

Barrie, L. A., Bottenheim, J. W., Schnell, R. C., Crutzen, P. J., and Rasmussen, R. A.: Ozone destruction and photochemical reactions at polar sunrise in the lower Arctic atmosphere, Nature, 334, 138–141, 1988. 11052

Domine, F., Sparapani, R., Ianniello, A., and Beine, H. J.: The origin of sea salt in snow on Arctic sea ice and in coastal regions, Atmos. Chem. Phys., 4, 2259–2271, 2004. 11053

Domine, F., Taillandier, A. S., Simpson, W. R., and Severin, K.: Specific surface area, density and microstructure of frost flowers, Geophys. Res. Lett., 32, L13502, doi:10.1029/2005GL023245, 2005. 11054, 11059

Draxler, R. and Rolph, G.: HYSPLIT (HYbrid Single-Particle Lagrangian Integrated Trajectory) Model access via NOAA ARL READY Website, url-http://www.arl.noaa.gov/ready/hysplit4.html, 2003. 11054

Eicken, H., Krouse, H. R., Kadko, D., and Perovich, D. K.: Tracer studies of pathways and rates of meltwater transport through Arctic summer sea ice, J. Geophys. Res., 107, 8046, doi:10.1029/2000JC000583, 2002. 11060

Fan, S.-M. and Jacob, D. J.: Surface ozone depletion in Arctic spring sustained by bromine reactions on aerosols, Nature, 359, 522–524, 1992. 11052

Foster, K. L., Plastridge, R. A., Bottenheim, J. W., Shepson, P. B., Finlayson-Pitts, B. J., and

Spicer, C. W.: The Role of Br2 and BrCl in Surface Ozone Destruction at Polar Sunrise, Science, 291, 471–474, 2001. 11053

Frieß, U., Hollwedel, J., König-Langlo, G., Wagner, T., and Platt, U.: Dynamics and chemistry of tropospheric bromine explosion events in the Antarctic coastal region, J. Geophys. Res., 109, D06305, doi:10.1029/2003JD004133, 2004. 11053, 11056

Hausmann, M. and Platt, U.: Spectroscopic measurement of bromine oxide and ozone in the high Arctic during Polar Sunrise Experiment 1992, J. Geophys. Res., 99, 25 399–25 413, 1994. 11056

Hoenninger, G. and Platt, U.: Observations of BrO and its vertical distribution during surface ozone depletion at Alert, Atmos. Env., 36, 2481–2490, 2002. 11056

Johannessen, O. M., Shalina, E. V., and Miles, M. W.: Satellite Evidence for an Arctic Sea Ice Cover in Transformation, Science, 286, 1937, doi:10.1126/science.286.5446.1937, 1999. 11060

Jones, A. E., Anderson, P. S., Wolff, E. W., Turner, J., Rankin, A. M., and Colwell, S. R.: A role for newly forming sea ice in springtime polar tropospheric ozone loss? Observational evidence from Halley Station, Antarctica, J. Geophys. Res., 111, D08306, doi:10.1029/2005JD006566, 2006. 11053, 11058

Kaleschke, L., Lüpkes, C., Vihma, T., Haarpaintner, J., Bochert, A., Hartmann, J., and Heygster, G.: SSM/I Sea Ice Remote Sensing for Mesoscale Ocean-Atmosphere Interaction Analysis, Can. J. Rem. Sens., 27, 526–537, 2001. 11054

Kaleschke, L., Richter, A., Burrows, J., Afe, O., Heygster, G., Nothold, J., Rankin, A. M., Roscoe, H. K., Hollowedel, J., Wagner, T., and Jacobi, H.-W.: Frost flowers on sea ice as a source of sea salt and their influence on tropophspheric halogen chemistry, Geophys. Res. Lett., 31, L16114, doi:10.1029/2004GL020655, 2004. 11053, 11054, 11055, 11058

Massom, R. A., Eicken, H., Haas, C., Jeffries, M. O., Drinkwater, M. R., Sturm, M., Worby, A. P., Wu, X., Lytle, V. I., Ushio, S., Morris, K., Reid, P. A., Warren, S. G., and Allison, I.: Snow on Antarctic sea ice, Rev. Geophys., 39, 413–445, 2001. 11060

McConnell, J. C., Henderson, G. S., Barrie, L., Bottenheim, J., Niki, H., Langford, C. H., and Templeton, E. M. J.: Photochemical bromine production implicated in Arctic boundary-layer ozone depletion, Nature, 355, 150–152, 1992. 11052

Overpeck, J. T., Sturm, M., Francis, J. A., Perovich, D. K., Serreze, M. C., Benner, R., Carmack, E. C., III, S. C., Gerlach, S. C., Hamilton, L. C., Hinzman, L. D., Holland, M., Huntington, H. P., Key, J. R., Lloyd, A. H., MacDonald, G. M., McFadden, J., Noone, D., Prowse, T. D.,

Sea ice, frost flowers and halogen activation

W. R. Simpson et al.

Title Page

Abstract	Introduction
Conclusions	References
Tables	Figures

|◄ | ►|

◄ | ►

Back | Close

Full Screen / Esc

Printer-friendly Version

Interactive Discussion

EGU

Schlosser, P., and Vörösmarty, C.: Arctic System on Trajectory to New, Seasonally Ice-Free State, Eos Trans. AGU, 86, 309, 2005. 11060

Perovich, D. and Richter-Menge, J. A.: Surface characteristics of lead ice, J. Geophys. Res., 99, 16 341–16 350, 1994. 11054, 11059

5 Rankin, A. M., Wolff, E. W., and Martin, S.: Frost flowers: Implications for tropospheric chemistry and ice core interpretation, J. Geophys. Res., 107, 4683–4694, 2002. 11053, 11059

Schroeder, W. H., Anlauf, K. G., Barrie, L. A., Lu, J. Y., Steffen, A., Schneeberger, D. R., and Berg, T.: Arctic springtime depletion of mercury, Nature, 394, 331–332, 1998. 11052

Serreze, M. C., Maslanik, J. A., Scambos, T. A., Fetterer, F., Stroeve, J., Knowles, K., Fowler, 10 C., Drobot, S., Barry, R. G., and Haran, T. M.: A record minimum arctic sea ice extent and area in 2002, Geophys. Res. Lett., 30, 1110, doi:10.1029/2002GL016406, 2003. 11060

Simpson, W. R., Alvarez-Aviles, L., Douglas, T. A., Sturm, M., and Domine, F.: Halogens in the coastal snow pack near Barrow, Alaska: Evidence for active bromine air-snow chemistry during springtime, Geophys. Res. Lett., 32, L04811, doi:10.1029/2004GL021748, 2005. 11053

15 Stroeve, J. C., Serreze, M. C., Fetterer, F., Arbetter, T., Meier, W., Maslanik, J., and Knowles, K.: Tracking the Arctic's shrinking ice cover: Another extreme September minimum in 2004, Geophys. Res. Lett., 32, L04501, doi:10.1029/2004GL021810, 2005. 11060

Sturm, M., Holmgren, J., and Perovich, D. K.: The winter snow cover of the sea ice of the Arctic Ocean at SHEBA: Temporal evolution and spatial variability., J. Geophys. Res., 107, 8047, 20 doi:10.1029/2000JC000400, 2002. 11060

Tuckermann, M., Ackermann, R., Golz, C., Lorenzen-Schmidt, H., Senne, T., Stutz, J., Trost, B., Unold, W., and Platt, U.: DOAS-observation of halogen radical-catalysed arctic boundary layer ozone destruction during the ARCTOC campaigns 1995 and 1996 in Ny-Alesund, Spitsbergen, Tellus, 49B, 533–555, 1997. 11057

25 Voss, S., Heygster, G., and Ezraty, R.: Improving sea ice type discrimination by the simultaneous use of SSM/I and scatterometer data, Polar Res., 22, 35–42, 2003. 11056

Wagner, T., Leue, C., Wenig, M., Pfeilsticker, K., and Platt, U.: Spatial and temporal distribution of enhanced boundary layer BrO concentrations measured by the GOME instruments aboard ERS-2, J. Geophys. Res., 106, 24 225–24 235, 2001. 11053

Title Page

Abstract | Introduction

Conclusions | References

Tables | Figures

◄ | ►►

◄ | ►

Back | Close

Full Screen / Esc

Printer-friendly Version

Interactive Discussion

EGU
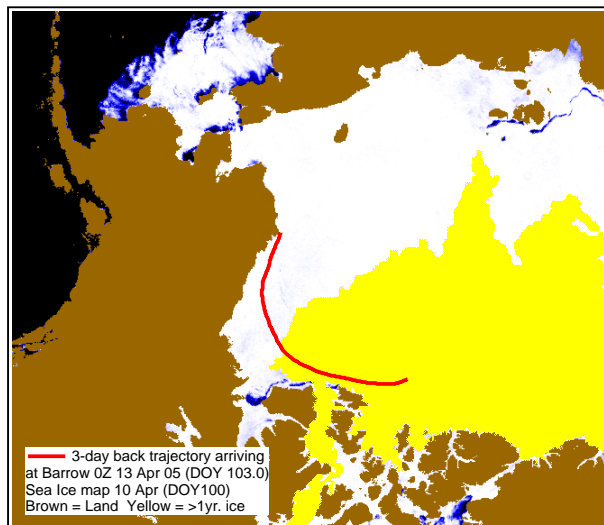
Fig. 1. An example of a 3-day back trajectory arriving at Barrow, Alaska. The arrival time is 00:00 UTC on 13 April 05 (DOY 103.0). The sea-ice map is shown for 10 April because the main contact of these trajectories with open water occurred on that day. The proper sea-ice map is used for each day of the trajectory calculation. The ice map shows brown for land, a gradation from black to white via blue tones for ice concentration, from AMSR-E data, and yellow for the area identified as multi-year ice from QuikSCAT sea ice age estimations.
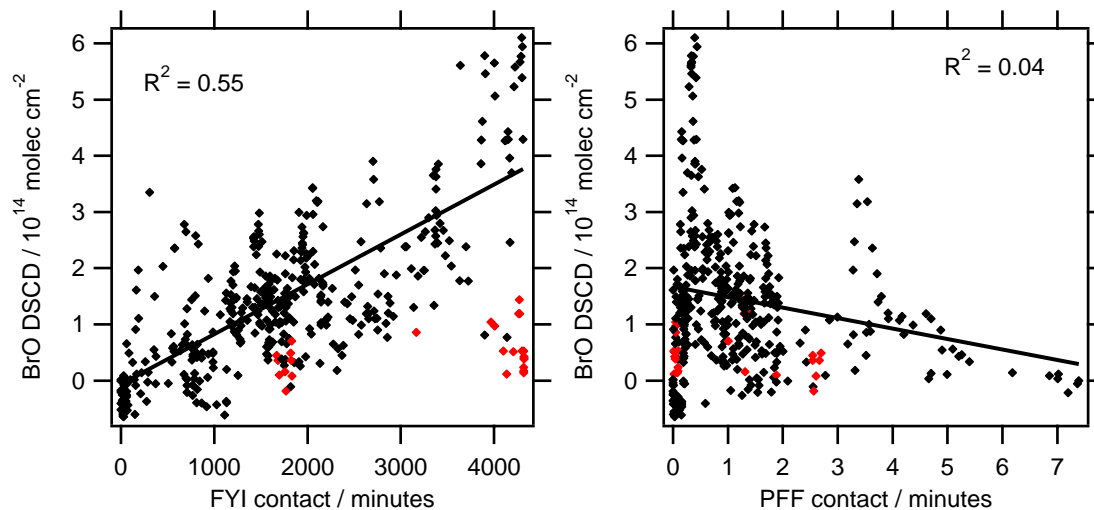
EGU
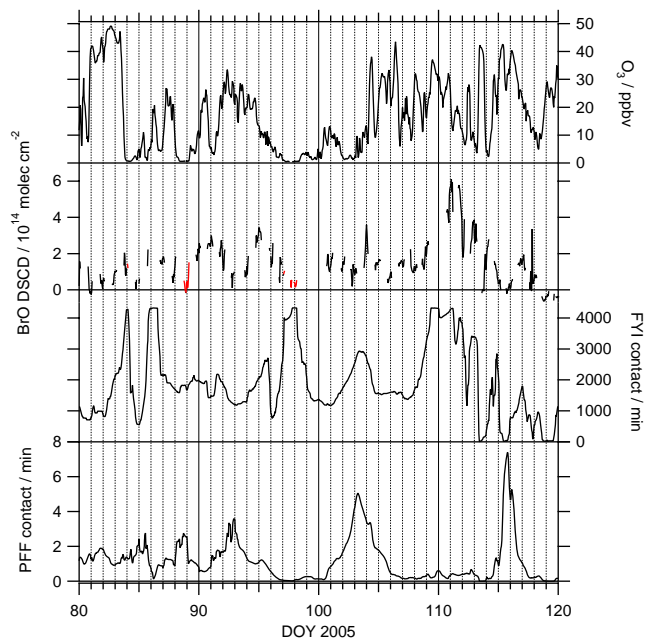
Fig. 2. Ozone, Bromine monoxide (BrO), first-year sea-ice contact (FYI), and potential frost flowers contact (PFF) timeseries in the period DOY 80–120. BrO data colored red occurred when ozone <1 ppbv.

Fig. 3. Correlation plots of BrO versus first-year sea-ice contact (left) and potential frost flowers contact (right). Data colored in red occurred when ozone <1 ppbv and were ignored from the correlation analysis.

EGU